Modeling Studies of Transport Bifurcation in the Drift Wave Turbulent Plasma of CSDX

R. J. Hajjar, P. H. Diamond, A. Ashourvan, G. R. Tynan

Mechanical and Aerospace Engineering Department
University of California, San Diego

Abstract

Self-organization of drift wave turbulence via particle flux and Reynolds stresses is now widely considered as a mechanism for turbulence suppression and cross field transport reduction. This energy transfer mechanism between microscale drift waves and mesoscale zonal flows creates a plasma transport bifurcation that triggers the formation of internal transport barriers, often associated with L→H transitions. We report here on some studies performed while investigating the transport bifurcation dynamics in CSDX linear device using a 1D reduced turbulence and mean field evolution model. This two-mixing scales Hasegawa-Wakatani based model evolves spatio-temporal variations of three plasma fields: the mean density n, the mean vorticity u and the turbulent potential enstrophy e. The model adopts inhomogeneous potential vorticity mixing on a mixing length which expression is related to the Rhines' scale (i.e. is ∇n and ∇u dependent). The model also uses expressions of the turbulent fluxes of n, u and e derived from the mixing length concepts. Particle and enstrophy turbulent fluxes are written as purely diffusive fluxes, while a residual stress part is added to the diffusive term in the expression of the vorticity flux. Mixed boundary conditions are used at both edges of our domain. Simulation results show a steepening in the particle density profiles along with the formation of a net flow shear layer resulting from the vorticity mixing. These results suggest the existence of system dynamics capable of sustaining the plasma core by means of a purely diffusive particle flux, without any explicit inward particle pinch.

1-What are we doing?

- Model the transport bifurcation observed in CSDX in an attempt to recover and numerically verify the experimental results.

- Confirm the existence of turbulence suppression in linear devices, specifically in CSDX, and verify its leading role in the generation of mean flow shear via the Reynolds work coupling mechanism, and in the formation of transport barrier as a route to enhanced confinement.

2-Why do we care?

- Such an investigation allows for a better understanding of how transport barriers are triggered and how a possible $L \rightarrow H$ transition is initiated.

3-<u>How</u> to do so?

- Use of **1D time dependent reduced** transport model, that evolves the three plasma fields: mean density **<*n*>**, mean vorticity **<*u*>** and turbulent potential enstrophy ***ε***.

- The model is based on the Modified Hasegawa-Wakatani model, and adopts inhomogeneous vorticity mixing.

4-<u>What</u> is new in this model?

- Our model is a **purely diffusive** one and **does not include any inward particle pinch** in the expressions of turbulent fluxes of density, vorticity and enstrophy.

- The model assumes a conservation of the total potential enstrophy (mean + turbulent PE) up to dissipation and external forcing effects.

- PV mixing occurs on a nonlinear mixing length that is related to l_{Rh} and shrinks as ∇n and ∇u steepen.

Tell me the Story…

Experimental results

- A **transport bifurcation** was recovered in CSDX as a result of an increasing magnetic field above $B_{cr}=1200G$. This bifurcation correlates with the following observations:

1. Steepening of the density profile .
2. Radially sheared azimuthal flow .
3. Fluctuation driven inward particle flux right at the location of the plasma density steepening.

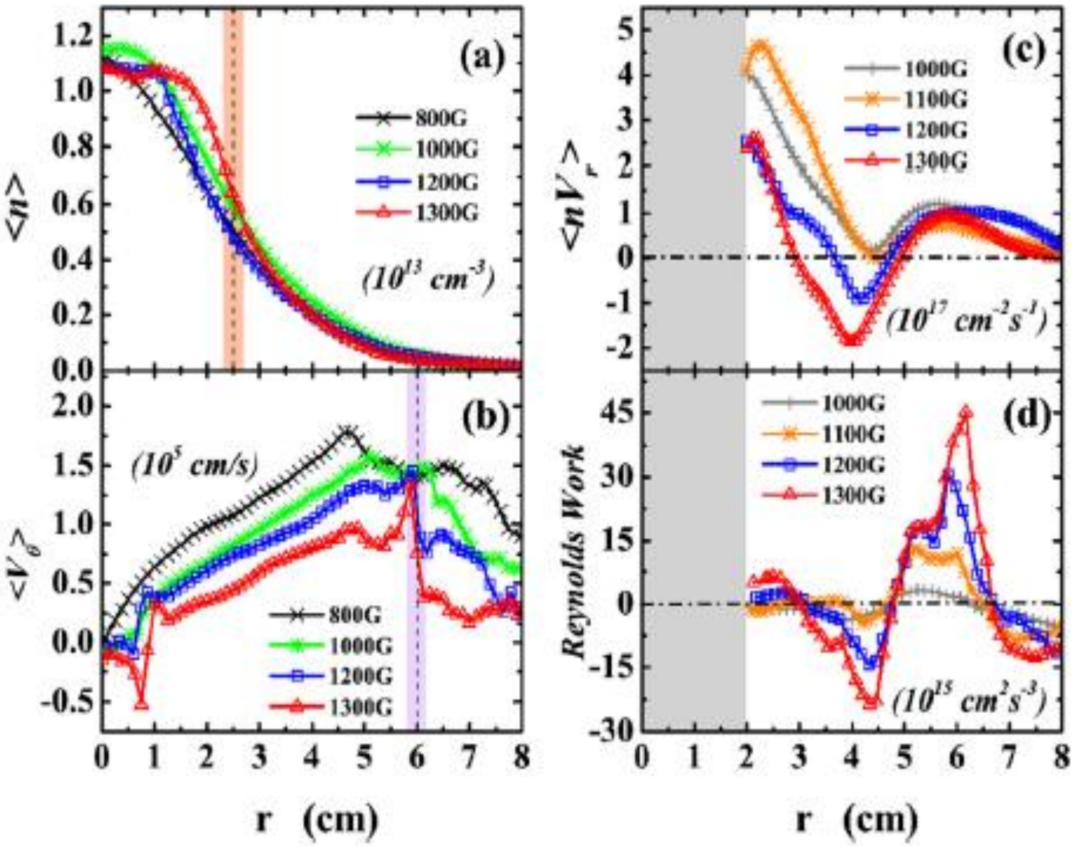

a) Cui L. *et al*, PoP **22**, 050704 (2015)
b) Cui L. *et al*, PoP **23**, 055704 (2016)

Experimental results

4. Negative Reynolds work values indicating a turbulence suppression and an energy transfer from fluctuating structures to the mean flow.

5. A total Reynolds work $\int -\frac{\partial \langle \tilde{V}_x \tilde{V}_y \rangle}{\partial x} . \bar{V}_y dx$ that is proportional to $1/L_n$, showing that the density steepening is correlated with turbulence suppression and work on the mean flow.

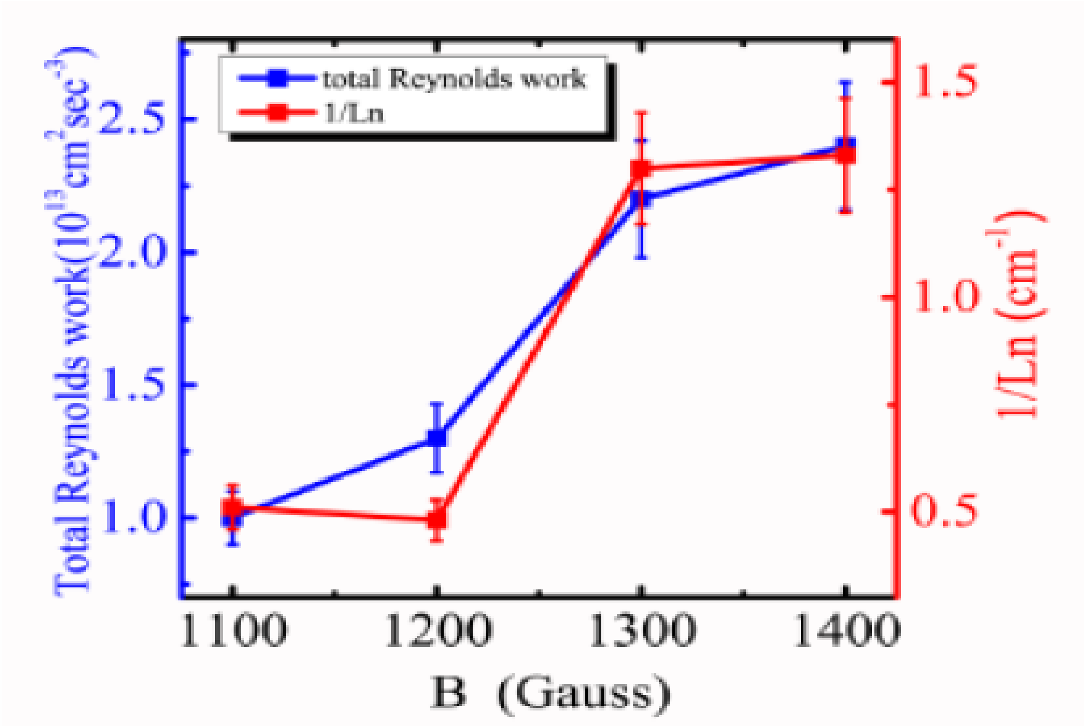

Background

- Sheared flows important role in regulating the multi-scale interaction between turbulent fluctuations and mean fields. This role is well established theoretically, experimentally and numerically.

- Formulation of several predator-prey models that describe the energy interplay between disparate scales structures and verify:

  1- Production of a non-zero Reynolds stress leading to ZF self organization from a standpoint of a vorticity transport according to a backward energy cascade.

  2- Enhancement of small scale fluctuations decorrelation which regulates turbulence and reduces transport via a forward enstrophy cascade.

- Drop in turbulence intensity = reduction of heat flux across the flux surfaces = formation of transport barriers crucial for higher confinement states.

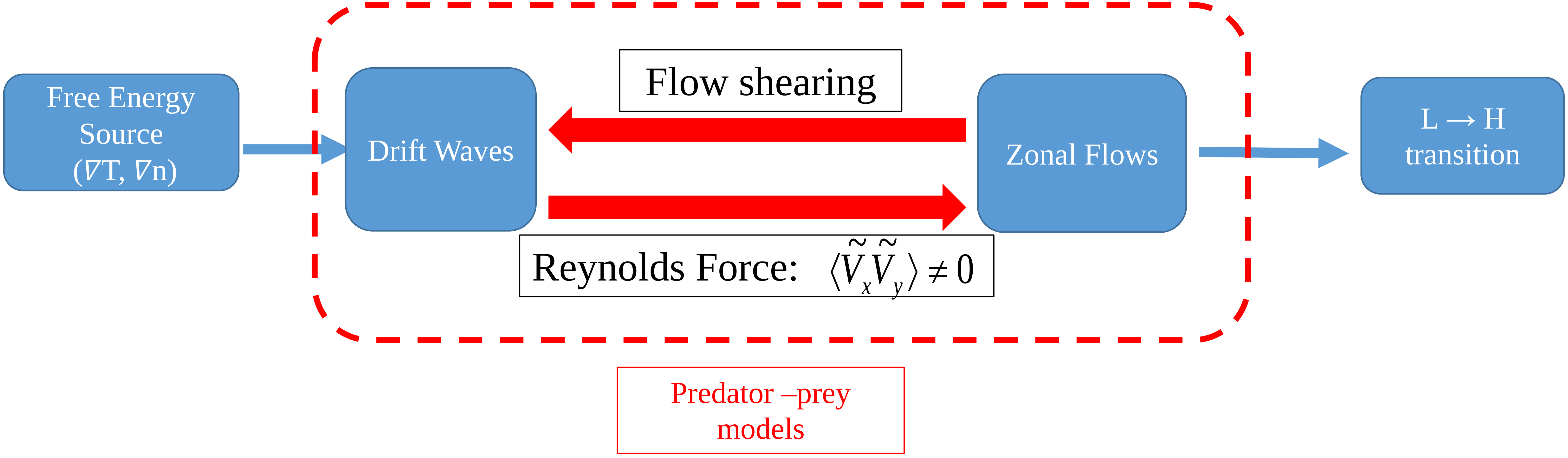
Free Energy Source (∇T, ∇n)
Drift Waves
Flow shearing
Zonal Flows
L → H transition
Reynolds Force: $\langle \tilde{V}_x \tilde{V}_y \rangle \neq 0$
Predator –prey models

The model

- This flux driven model explains the reduction of the global vorticity gradient and the acceleration of zonal flows by PV mixing.
- Using quasi-linear theory, in the near adiabatic regime, the expressions of the adopted turbulent fluxes are:

$$\Gamma_n = -D_n \partial_x \langle n \rangle + V_{pinch} \langle n \rangle$$

$$\Gamma_\varepsilon = -D_\varepsilon \partial_x \varepsilon$$

$$\Pi = (\chi - D_n)\partial_x \langle n \rangle - \chi \partial_x \langle u \rangle = \Pi_{res} - \chi \partial_x \langle u \rangle$$

$$\Pi_{res} = \Gamma_n / n - \chi . v_d$$

- The Diffusion coefficients are of the form:

$$D_\alpha = \langle \varepsilon l_{mix}^2 \rangle \tau_C = \frac{\langle \varepsilon l_{mix}^2 \rangle}{\sqrt{\varepsilon + q^2 + (l_{mix} \nabla q)^2}} = \frac{\langle \varepsilon l_{mix}^2 \rangle}{\sqrt{\varepsilon + c_u u^2}}$$

The denominator represents:
1. Presence of a flow shear and a mean vorticity transport.
2. PV production rate (absent in our case)

Ashourvan A. *et al*, PoP, **23** 022309 (2016)

The mixing length

- l_{mix} has a hybrid expression: $$l_{mix}^2 = \frac{l_0^2}{1+(l_0/l_{Rh})^2} = \frac{l_0^2}{1+l_0^2(\nabla(n-u))^2/\varepsilon}$$

  where l_0 and l_{Rh} and the macroscopic mode scale (external forcing dimension) and the microscopic Rhines' scale of turbulence respectively.

- Alternative forms of the mixing length include:

  - $l_{mix} \sim l_0$ when vorticity gradient is weak, i.e. perturbations of a vortex immersed in a weak ambient strain generated by other vortices.

  - $l_{mix} \sim l_{Rh}$ when PV gradient cannot be neglected, i.e. case of a strong turbulence and infinite Reynolds number.

- The Rhines' scale being $\nabla q = \nabla n - \nabla u$ dependent, l_{mix} is also inversely proportional to the PV gradient and shrinks and the latter decreases.

- This choice of l_{mix} promotes decorrelation of small scale structures and energy build up onto the *k=0* mode.
- It provides a closed feedback loop between ∇q and the PV mixing coefficient.
- The model presents a unique and exceptional opportunity to verify and investigate the turbulence transport in CSDX.

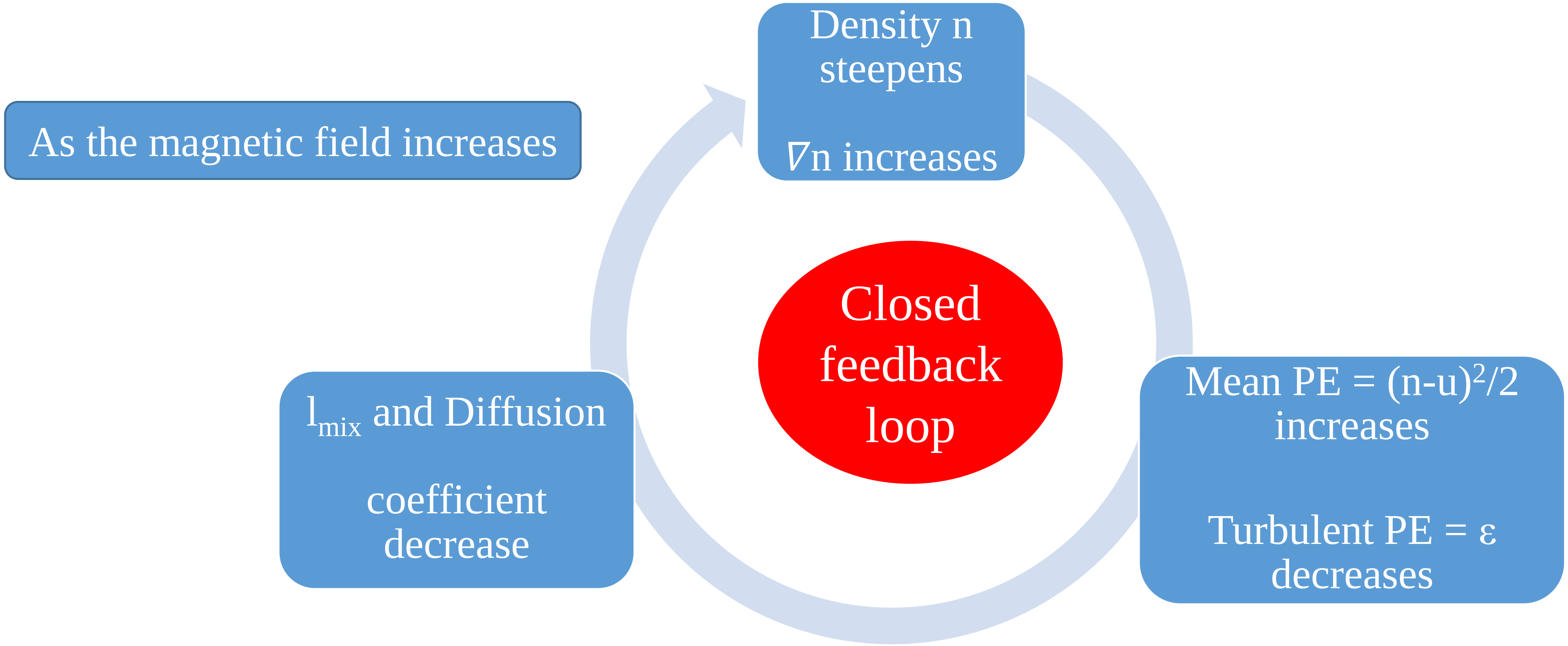

Case 1: Diffusive PV flux ($D_n=\chi$)

Turbulent Diffusion Terms

Classical diffusive and viscous terms

$$\omega_i \frac{\partial n}{\partial t} = \frac{\partial}{\partial x}\left[\frac{\varepsilon^{3/2} l_0^2}{\varepsilon + l_0^2(\partial_x(n-u/\rho_s^2))^2}\frac{\partial n}{\partial x} + D_c \frac{\partial n}{\partial x}\right] + S(x)$$

external source= synergy between neutrals and heating power

$$\omega_i \frac{\partial u}{\partial t} = \frac{\partial}{\partial x}\left[\frac{\varepsilon^{3/2} l_0^2}{\varepsilon + l_0^2(\partial_x(n-u/\rho_s^2))^2}\frac{\partial u}{\partial x} + \mu_c \frac{\partial u}{\partial x}\right]$$

$$\omega_i \frac{\partial \varepsilon}{\partial t} = \frac{\partial}{\partial x}\left[\frac{\varepsilon^{3/2} l_0^2}{\varepsilon + l_0^2(\partial_x(n-u/\rho_s^2))^2}\frac{\partial \varepsilon}{\partial x}\right] + L^2\left[\frac{l_0^2\varepsilon^{3/2}(\partial_x(n-u/\rho_s^2))^2}{\varepsilon + l_0^2(\partial_x(n-u/\rho_s^2))^2}\right] - 2\varepsilon^{3/2} + \sqrt{\varepsilon}$$

ε internal production; coupling between n and u

ε dissipation

Forcing= external production

Model results

<u>Numerical techniques, initial profiles and boundary conditions</u>

- Mixed Boundary conditions are adopted:
  - DBC at x=1 and NBC at x=0 for *n* and *u*.
  - NBC at x=0 and x=1 for ε to ensure absence of energy input/output.
- We write S(x) as a Gaussian centered at $x_0=0.7$.
- $n(x,0)=(1-x)\,Exp[-ax^2+b]$; $u(x,0)=cx^2+dx^3$; $\varepsilon(x,0)=(n(x,0)-u(x,0))^2/2$

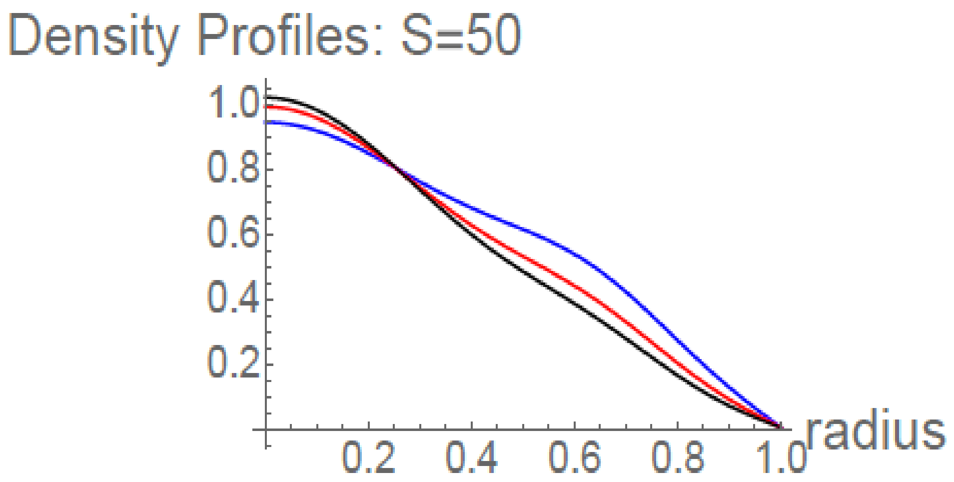

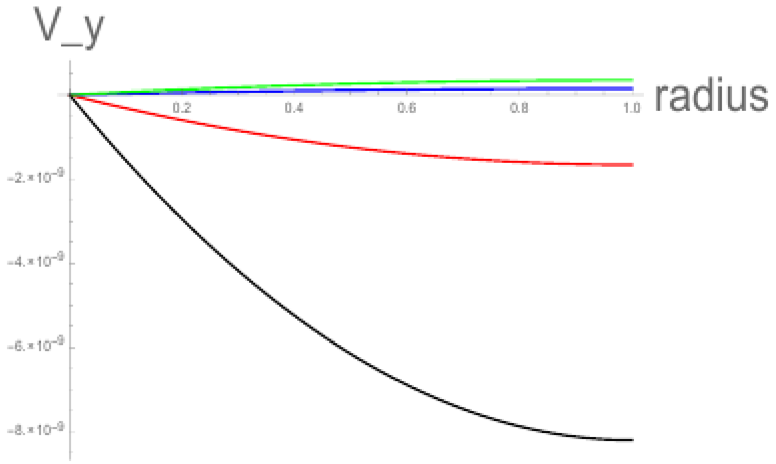

Model results

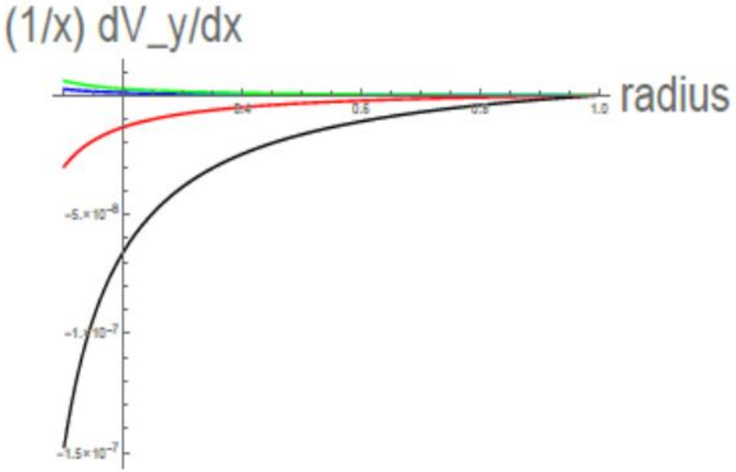

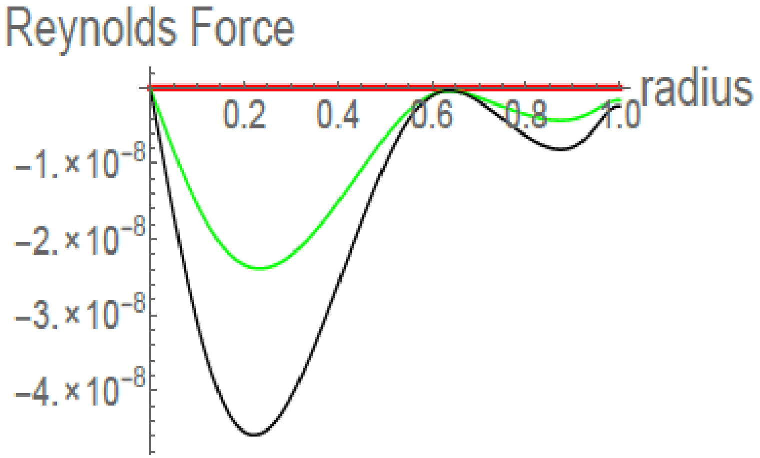

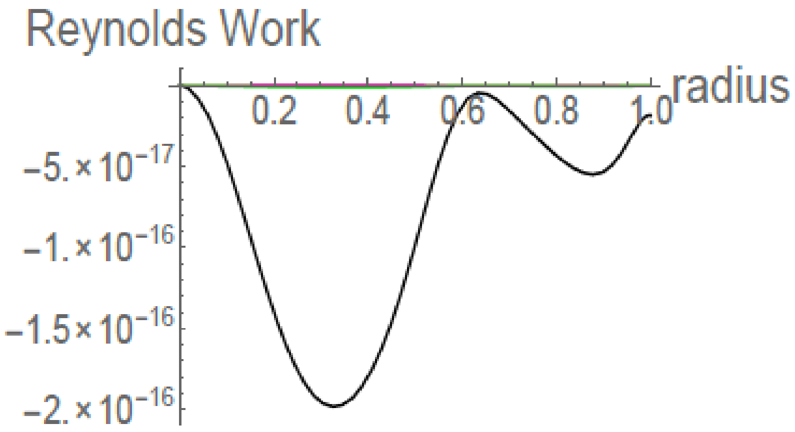

Observations:

- Steepening of n as *B* increases.
- Radially sheared azimuthal velocity. The shear layer coincides with the region of density steepening and intensifies as *B* increases.
- Negative Reynolds work indicating a turbulence suppression and a transfer of energy from turbulent structures to the mean flow (Rey. work= Rey. force times V_y).

Model results

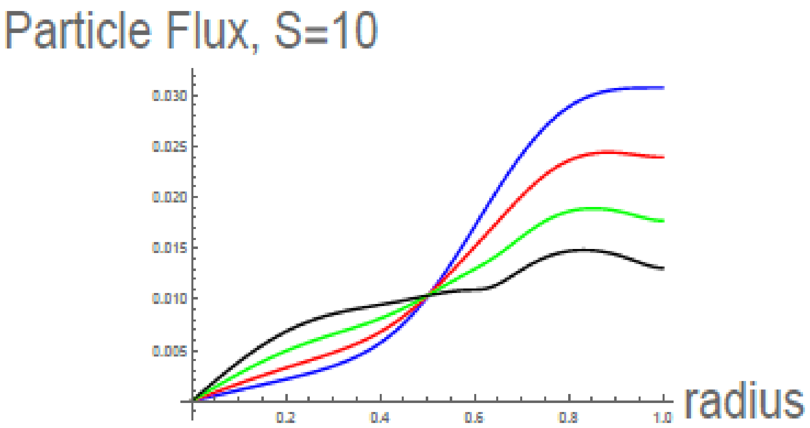

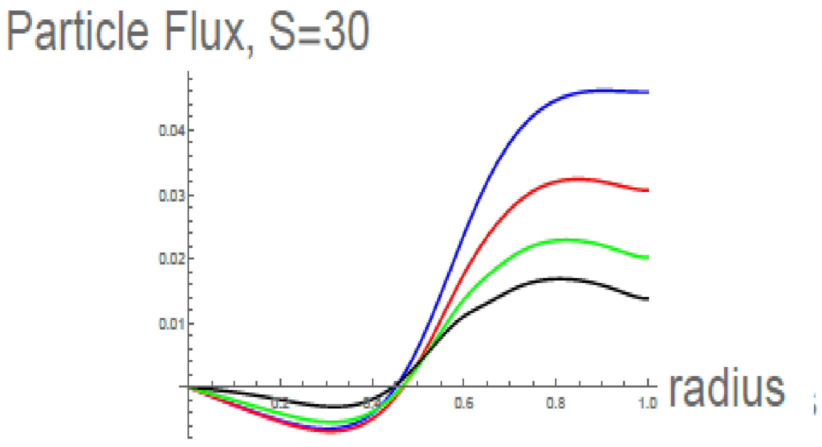

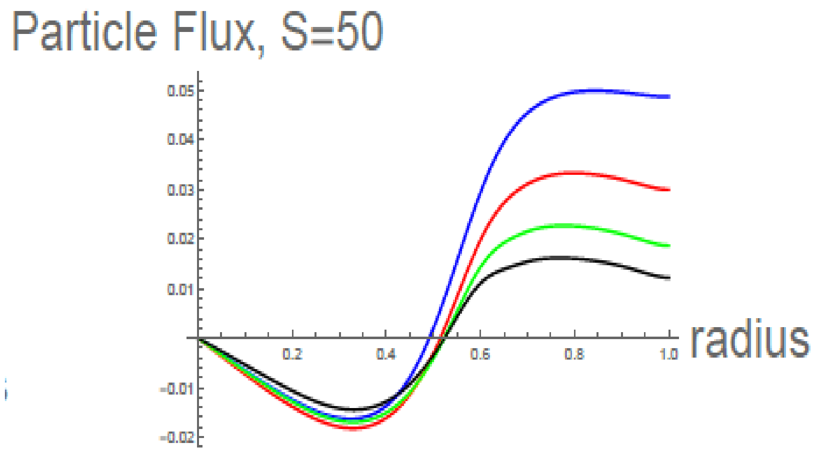

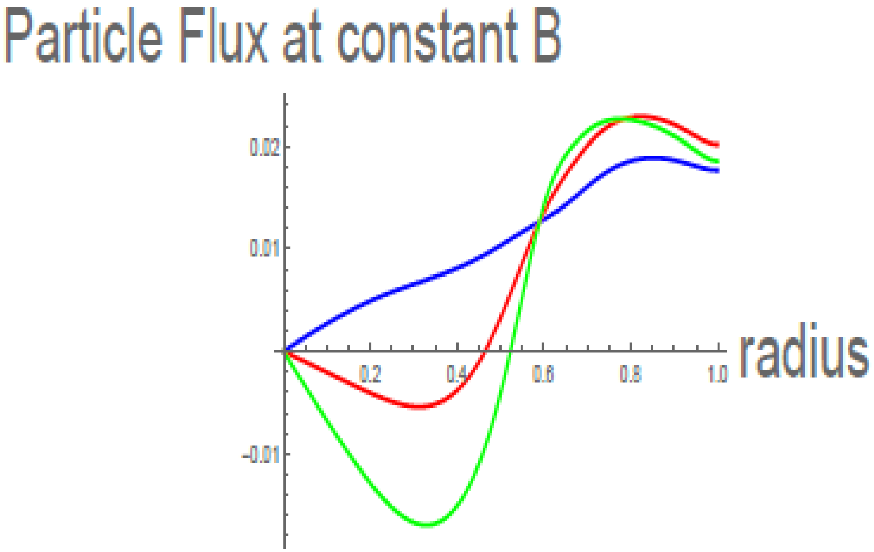

- The inward particle flux reported experimentally to be inherent to the system, seems to be crucially dependent on the fueling intensity *S*.
- *Additional investigation of available data is needed.*

Local validation metrics for the model

At the density steepening location, we calculate:

$$\frac{\Delta(1/L_n)}{L_{n_i}} = \frac{1/L_{n_f} - 1/L_{n_i}}{1/L_{n_i}} = \begin{cases} \sim 0.70 & \text{numerically} \\ \sim 0.55 & \text{experimemtally} \end{cases}$$

$$\frac{\Delta(1/L_v)}{L_{v_i}} = \frac{1/L_{v_f} - 1/L_{v_i}}{1/L_{v_i}} = \begin{cases} \sim 0.73 & \text{numerically} \\ \sim 0.57 & \text{experimentally} \end{cases}$$

Both experimental and numerical values of the relative variation of the density and velocity gradient scale length L_n and L_v are comparable.

Global validation metrics for the model

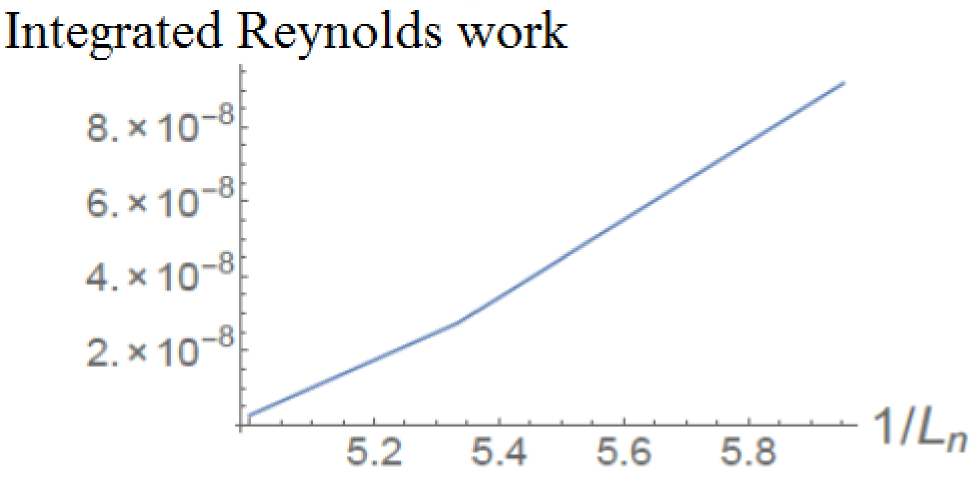

As *B* increases, the density profile steepens, $1/L_n$ increases and the total Reynolds work increases proportionally, indicating a turbulence suppression.

$1/\tau_{loss}(\times 10^{-2})$	$S=10$	$S=30$	$S=50$
B_{blue}	1.4	2.5	3.0
B_{red}	1.2	1.0	2.6
B_{black}	0.9	0.8	1.8

TABLE I: Particle loss rate $1/\tau$ for increasing B.

A surface integral of the particle flux along *r* gives values of the particle loss rates:

$$1/\tau_{loss} \propto \int r\Gamma_n dr$$

These decreases as B increases which indicates a change in the nature of turbulence of the system.

Case 2: PV flux includes a residual stress: $\Pi = \Pi_{res} - \chi \partial_x u$

For $D_n = l_{mix}^2 \frac{\varepsilon}{\alpha}$, $\chi = l_{mix}^2 \frac{\varepsilon}{\sqrt{\alpha^2 + c_u u^2}}$, $D_\varepsilon = l_{mix}^2 \varepsilon^{1/2}$, the system becomes:

$$\omega_i \frac{\partial n}{\partial t} = \frac{\partial}{\partial x}\left[\frac{l_0^2 \varepsilon^2}{\varepsilon + l_0^2(\partial_x(n - u/\rho_s^2))^2}\frac{\partial n}{\partial x}\frac{1}{\alpha} + D_c \frac{\partial n}{\partial x}\right] + S(x)$$

$$\omega_i \frac{\partial u}{\partial t} = \rho_s^2 \frac{\partial}{\partial x}\left[\frac{l_0^2 \varepsilon^2}{\varepsilon + l_0^2(\partial_x(n - u/\rho_s^2))^2}\left[\left(\frac{1}{\alpha} - \frac{1}{\sqrt{\alpha^2 + c_u(u/\rho_s^2)^2}}\right)\frac{\partial n}{\partial x} + \left(\frac{1}{\sqrt{\alpha^2 + c_u(u/\rho_s^2)^2}} + \mu_c\right)\frac{\partial u}{\partial x}\right]\right]$$

$$\omega_i \frac{\partial \varepsilon}{\partial t} = \frac{\partial}{\partial x}\left[\frac{l_0^2 \varepsilon^{3/2}}{\varepsilon + l_0^2(\partial_x(n - u/\rho_s^2))^2}\frac{\partial \varepsilon}{\partial x}\right] + L_0^2\left[\frac{l_0^2 \varepsilon^2 \rho_s}{\varepsilon + l_0^2(\partial_x(n - u/\rho_s^2))^2)}\left(-\frac{1}{\alpha} + \frac{1}{\sqrt{\alpha^2 + c_u(u/\rho_s^2)^2}}\right)\left(\frac{\partial n}{\partial x} - \frac{1}{\rho_s^2}\frac{\partial u}{\partial x}\right)\right.$$
$$\left. - \frac{l_0^2 \varepsilon^2}{\varepsilon + l_0^2(\partial_x(n - u/\rho_s^2))^2}\left(-\frac{1}{\alpha}\frac{\partial n}{\partial x} + \frac{1}{\sqrt{\alpha^2 + c_u(u/\rho_s^2)^2}}\frac{1}{\rho_s^2}\frac{\partial u}{\partial x}\right)\left(\frac{\partial n}{\partial x} - \frac{1}{\rho_s^2}\frac{\partial u}{\partial x}\right) - 2\varepsilon^{3/2} + \sqrt{\varepsilon}\right]$$

Model results

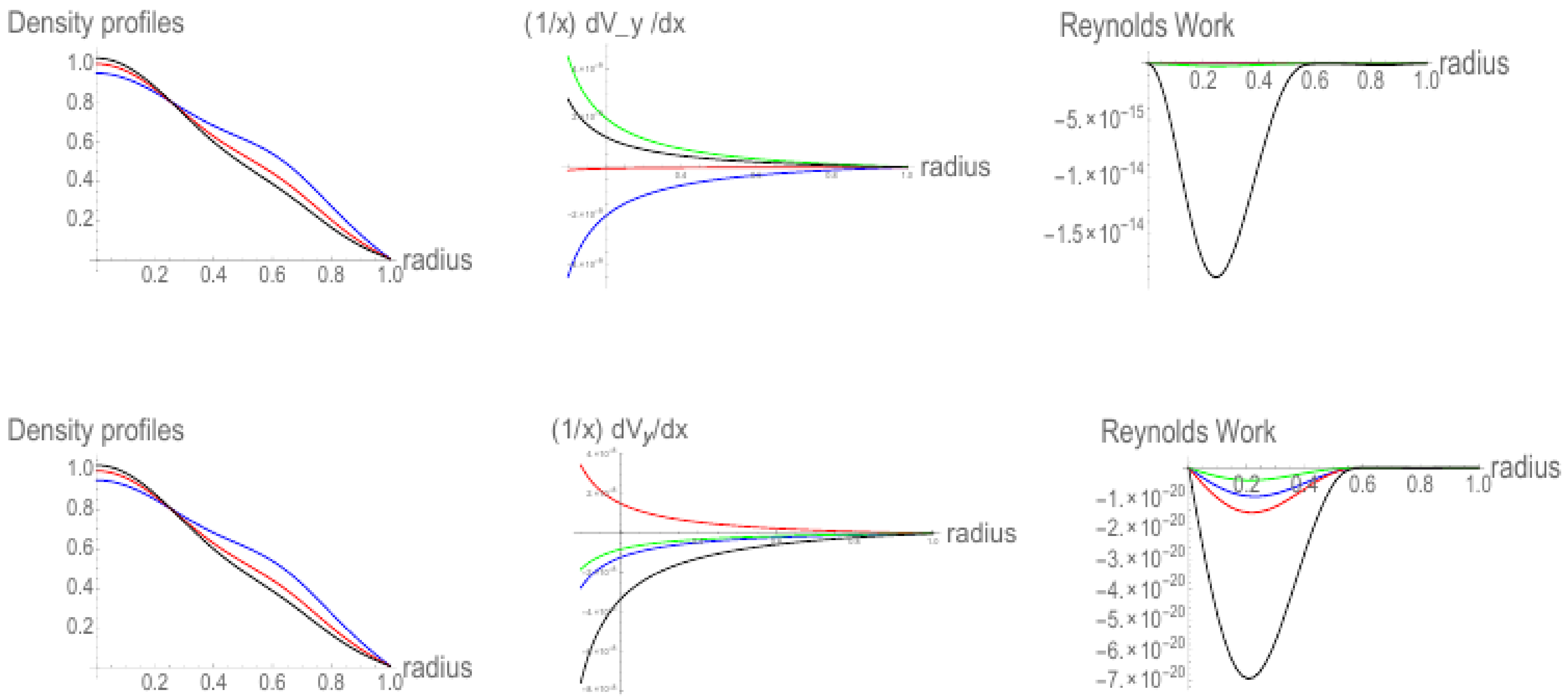

FIG. 9: Plasma profiles with Π_{res} and Dirichlet boundary conditions for $c_u = 6$ and $c_u = 600$ respectively ($B_{blue} < B_{red} < B_{green} < B_{black}$).

Model results

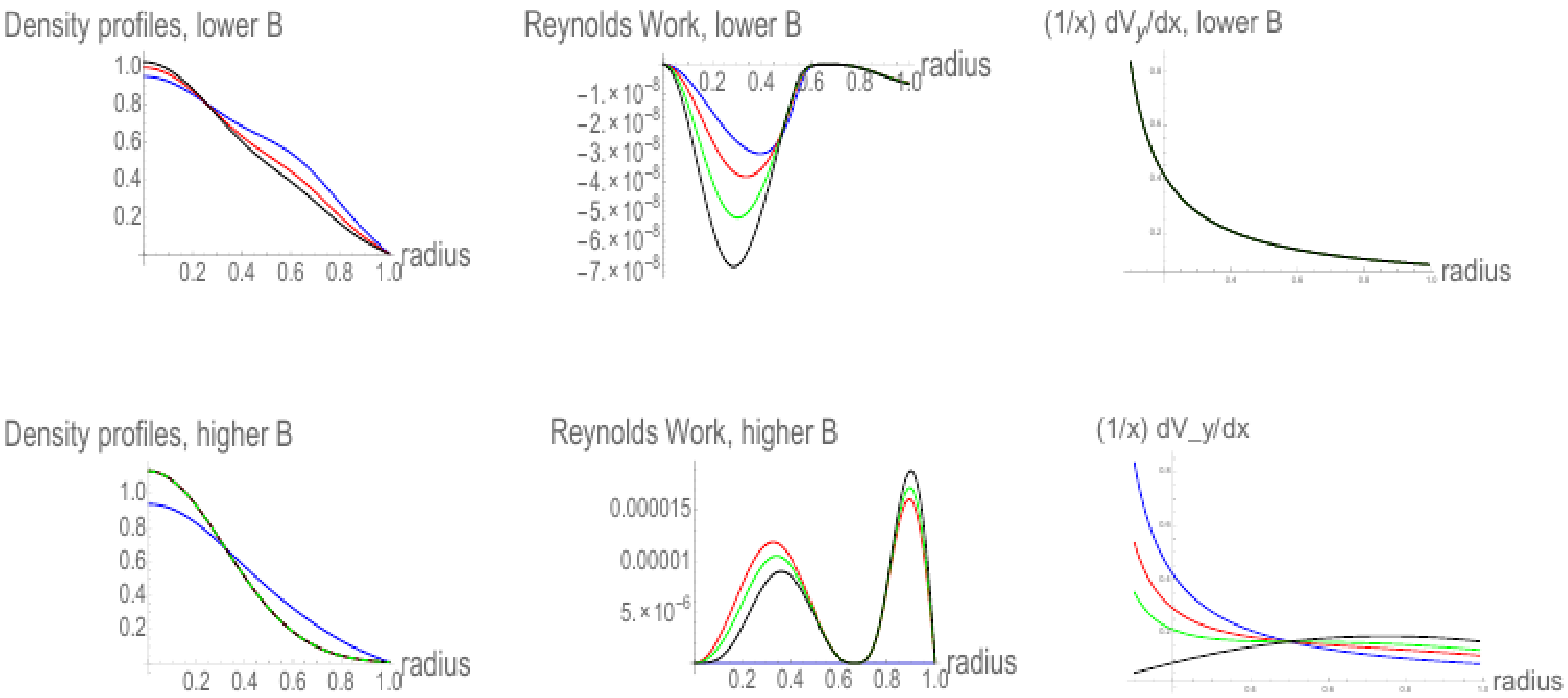

FIG. 10: Plasma profiles with Π_{res} and Neumann boundary conditions ($B_{blue} < B_{red} < B_{green} < B_{black}$).

Model results

- When a DBC is imposed on *u* at x=1, we recover the same observations reported previously: density steepening, formation of a shear layer and turbulence suppression, i.e., a transfer of energy form the turbulent fluctuations to the mean flow (slide 20).
- These observations do not seem to be qualitatively affected by the shear intensity c_u (not shown here)

- When a NBC is imposed at x=1 (unrealistic case of a plasma column surrounded by a thin neutral layer, where viscous effects are negligible), we recover the density steepening as well as the negative Reynolds work variations as *B* increases. The velocity shear however, although present right at the density steepening location, is *B* independent (slide 21 top figures).
- Larger values of *B* ($\sim 10^4$ $\times$ bigger) are required for this *B*-dependence to appear. The Reynolds work becomes positive, which indicates a turbulence promotion rather than suppression and a relaxation of the vorticity gradient (slide 21 bottom figures).

Energy Exchange: R_T

- Define the parameter R_T as the ratio of the rate of energy transfer from turbulence to the flow, to the rate of energy input into fluctuations.

$$R_T = \frac{\langle \tilde{V}_x \tilde{V}_y \rangle ' \overline{V}_{E\times B}}{\gamma_{eff} \langle \tilde{V}_\perp^2 \rangle}$$

$$\gamma_{eff} = \left| \frac{1}{\varepsilon} . \frac{\partial \varepsilon}{\partial t} \right|$$

$$\langle \tilde{V}_\perp^2 \rangle = \varepsilon . l_{mix}^2$$

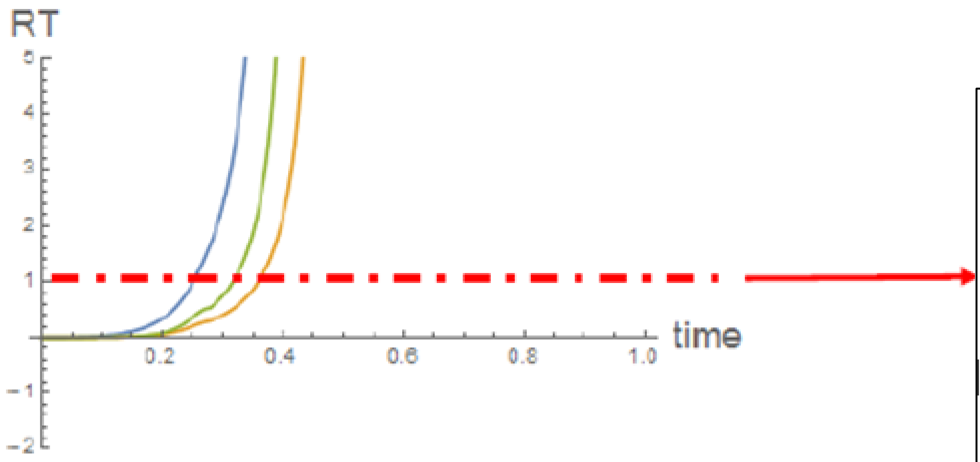

R_T vs time at x=0.1, 0.6 and 0.8 cm (blue, green, brown)

When R_T>1, the flow extracts energy from the turbulence faster than Turbulent Kinetic Energy grows:

- Turbulence collapse and suppression
- Formation of a transport barrier as a necessary keystone for the $L \rightarrow H$ transition

Beyond R_T: R_{DT}

- Direct experimental measurements of R_T, equivalently defined as:

$$R_T = \frac{\langle \tilde{V}_x \tilde{V}_y \rangle . \overline{V}'_{ExB}}{\nu_{net} . \langle \tilde{V}_\perp^2 \rangle}$$

where ν_{net} is the effective rate of energy input into the turbulence, were performed in EAST tokamak. Measurements showed that an $L \rightarrow H$ transition was triggered as soon as R_T exceeded order unity.

- RT has the following issues:

  - vague definition of γ_{eff}

  - why are we only considering the turbulent Kinetic Energy $\langle \tilde{V}_\perp^2 \rangle$

- To avoid ambiguity, we compare the Reynolds work (which is the energy coupled to the flow) to the total entropy production (which is the energy input due to density gradient relaxation).

Beyond R_T: R_{DT}

- We define a new parameter R_{DT}:

$$R_{DT} = \frac{-\int \Pi.\nabla u}{-\int \Gamma_n.\nabla n} = \frac{\int \partial_x^2 \langle \tilde{V}_x \tilde{V}_y \rangle u}{-\int \Gamma_n.\nabla n} = \frac{\text{Integrated enstrophy destruction due to vorticity coupling: negative energy transfer from turbulence to flow.}}{\text{Integrated enstrophy production related to density gradient relaxation: positive energy input from the density profile.}}$$

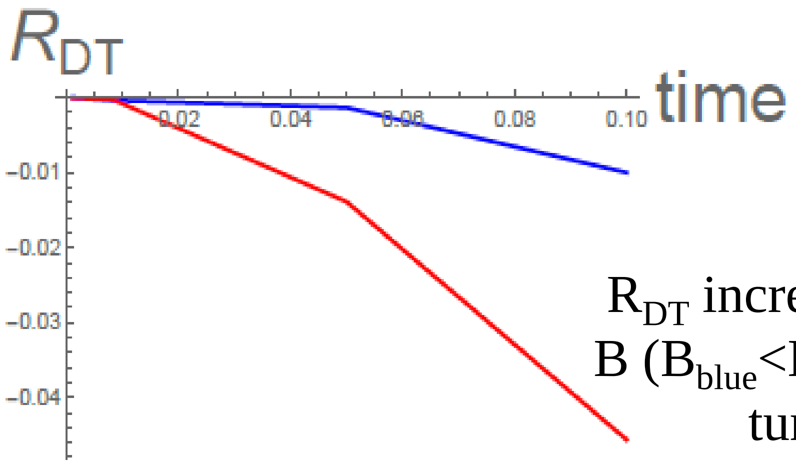

R_{DT} increases in absolute value with B (B_{blue}<B_{red}) as an additional sign of turbulence suppression

R_{DT} is easily measurable and determined numerically, it is superior to R_T and is a parameter to use as a turbulence collapse indicator. We note that this definition is limited to this model. For an L-H transition in tokamaks, a broader definition including a temperature gradient instead of the density gradient should be used

Conclusion

- Using a 1D time dependent reduced model, we were able to recover the transport bifurcation observed in CSDX.
- The model is simple and minimal: it is purely diffusive and there is no need for any inward particle and velocity pinch to recover the experimental observations.
- The choice of the PV mixing length is essential to close the loop between the PV gradient and the diffusion coefficient.
- Global and local verification of the turbulence suppression in CSDX and of the energy transfer from the DW fluctuations to the ZF structures.
- R_{DT} emerges as a superior turbulence collapse indicator in linear devices.

Future work

- Need to understand vorticity gradient relaxation reposted for a NBC and high *B*.
- Need to look for a dimensionless parameter which underlies the critical value of *B* that defines the plasma bifurcation.

Rhines' Scale

- Unlike the 3D turbulence case where vortex stretching leads to a *forward energy cascade* that drives fluid energy to smaller scales until being dissipated, in **2D** turbulence, vortex merging is inhibited via ***inverse energy cascade***.

- l_{Rh} separates the turbulence dominated regime from a wave-like behavior dynamics in the system.
- Eddy turnover rate = DW frequency.

$$1/\tau_c = \omega$$

$$\sqrt{\varepsilon} \approx l_{Rh} \nabla (n-u)$$

$$\boxed{l_{Rh} = \sqrt{\varepsilon} / \nabla (n-u)}$$